Advances in Materials Research, *Vol. 8, No. 3 (2019) 237-257*
DOI: https://doi.org/10.12989/amr.2019.8.3.237

Analyzing large-amplitude vibration of nonlocal beams made of different piezo-electric materials in thermal environment

Ahmed K. Muhammad, Luay Badr Hamad, Raad M. Fenjan and Nadhim M. Faleh*

Al-Mustansiriah University, Engineering Collage P.O. Box 46049, Bab-Muadum, Baghdad 10001, Iraq

(*Received September 6, 2019, Revised October 23, 2019, Accepted December 30, 2019*)

Abstract. The present article researches large-amplitude thermal free vibration characteristics of nonlocal two-phase piezo-magnetic nano-size beams having geometric imperfections by considering piezoelectric reinforcement scheme. The piezoelectric reinforcement can cause an enhanced vibration behavior of smart nanobeams under magnetic field. All previous studies on vibrations of piezoelectric-magnetic nano-size beams ignore the influences of geometric imperfections which are crucial since a nanobeam is not always ideal or perfect. Nonlinear governing equations of a smart nanobeam are derived based on classical beam theory and an analytical trend is provided to obtain nonlinear vibration frequency. This research shows that changing the volume fraction of piezoelectric phase in the material has a great influence on vibration behavior of smart nanobeam under electric and magnetic fields. Also, it can be seen that nonlinear vibration behaviors of smart nanobeam is dependent on the magnitude of exerted electric voltage, magnetic imperfection amplitude and substrate constants.

Keywords: piezo-magnetic nanobeam; geometrical imperfection; thermal vibration; piezoelectric reinforcement; electric voltage

1. Introduction

A type of multi phases smart materials known as magneto-electro-thermo-elastic (METE) material represents superb possible application in smart structures/systems as well as nano-sized devices owning to giving wonderful mechanical, electrical and magnetic coupling performances (Ebrahimi and Barati 2017). Applying electro-magnetic fields to METE nano-dimension beams yields elastic deformations and changed vibrational properties. Due to the reason that performing experiment on nano-dimension beams are effortful yet, many scholars have represented their theoretical models taking into account small scales influences (Zenkour and Sobhy 2015, Mashat *et al*. 2016, Sobhy and Abazid 2019, Sobhy and Zenkour 2018a-c, Mirjavadi *et al*. 2017, 2018a, b, 2019a-f, Azimi *et al*. 2017, 2018). Employing nonlocal theory of elasticity (Eringen 1972), one may be able to incorporate the small scales influences in theoretical model of nano-dimension beams (Thai and Vo 2012, Eltaher *et al*. 2012, 2016, Semmah *et al*. 2014, Zemri *et al*. 2015, Berrabah *et al*. 2013, Bounouara *et al*. 2016, Bouafia *et al*. 2017, Besseghier *et al*. 2017, Ebrahimi *et al*. 2017, Ahmed *et al*. 2019, Zenkour and Sobhy 2013, Alzahrani *et al*. 2013, Sobhy 2014a-b, 2015, 2019, Sobhy and Radwan 2017). The theory recommends a scale factor called nonlocal

*Corresponding author, Professor, E-mail: dr.nadhim@uomustansiriyah.edu.iq

http://www.techno-press.org/?journal=amr&subpage=5 ISSN: 2234-0912 (Print), 2234-179X (Online)

parameter for describing that the stress fields at nano scales have a nonlocal character (Ansari *et al*. 2012, Fang *et al*. 2013, Chen *et al*. 2014, Karličić *et al*. 2018, Barati and Zenkour 2017).

There are many published articles on vibrational analysis of piezo-magnetic nanoscale beams based on nonlocal theory of elasticity and different beam theories. Using nonlocal theory, an investigation of low amplitude free vibrational properties of smart nano-size beam made of METE material has been carried out by Ke and Wang (2014). In a research, Jandaghian and Rahmani (2016) represented linearly type free vibrational study of magneto-electrically loaded nano-size beams embedded on elastic substrates. Providing exact solutions, Ebrahimi and Barati (2017) researched vibrational characteristics of nonlocal METE nano-size beams having functionally graded material distribution. Large amplitude vibrations of METE nano-size beams using a numerical approach have been studied by Ansari *et al*. (2015). Moreover, damping effects due to viscoelasticity on vibrational characteristics of nano-scale beams made of magneto-electric material have been researched by Ebrahimi and Barati (2016).

The multi phases composite constructed by piezoelectric and piezo-magnetic constituents exhibits magneto-electrical influences which are invisible in single phase piezo-electrical and piezo-magnetic constituents (Nan 1994). Giving topmost mechanical efficiency under electrical and magnetic fields, a magneto-electro-elastic (MEE) material may be defined as a species of smart material having different application in sensing apparatus, smart systems and structural components (Aboudi 2001). Exposing to an exterior mechanical loading, a MEE material is capable to render electrical-magnetic field sensing (Li and Shi 2009, Arefi and Zenkour 2016, Guo *et al*. 2016, Pan and Han 2005). Furthermore, under electro-magnetic fields, such material experiences elastic deformations. For example, $BaTiO_3$ and $CoFe_2O_4$ may be composed to each other for creating a composite of MEE materials. According to the percentages of the two constituents, it is feasible to define material properties of the composite such as elastic moduli and piezo-magnetic constants. It is shown by other authors that vibration frequency of MEE structures is sensitive to the percentage of piezoelectric phase and hence vibration behavior of MEE can be controlled by varying the material composition (Kumaravel *et al*. 2007, Annigeri *et al*. 2007).

In this paper, analysis of nonlinear vibration behavior of multi-phase magneto-electro-thermo-elastic (METE) nano-size beams has been presented considering geometric imperfection effects. Multi-phase METE material is composed form piezoelectric and piezo-magnetic constituents for which the material properties can be controlled based on the percentages of the constituents. Nonlinear governing equations of METE nanobeam are derived based on nonlocal elasticity theory together with classic thin beam model and an approximate solution is provided. It will be shown that nonlinear vibrational behavior of METE nanobeam in electro-magnetic field depends on the constituent's percentages. Vibration frequency of METE nanobeam is also affected by nonlocal scale factor, magnetic field intensity and electrical voltage.

2. Magneto-electro-elastic composites with two phases

For two-phase MEE composites, all material characteristics are associated with the portion (volume fraction) of piezoelectric constituent (V_f). In the present paper, the nanobeam is made of piezo-magnetic $BaTiO_3$-$CoFe_2O_4$ material and Table 1 represents material coefficients. In this material, $BaTiO_3$ is the piezoelectric constituent and then $CoFe_2O_4$ is the piezo-magnetic constituent. Table 1 respectively defines elastic (C_{ij}), piezoelectric (e_{ij}) and piezo-magnetic (q_{ij}) properties. Moreover, k_{ij}, d_{ij} and x_{ij} respectively denote dielectric, magnetic-electric-elastic and

Table 1 Material properties of $BaTiO_3$-$CoFe_2O_4$ composites

Property	$V_f = 0$	$V_f = 0.2$	$V_f = 0.4$	$V_f = 0.6$	$V_f = 0.8$
C_{11} (GPa)	286	250	225	200	175
C_{13}	170	145	125	110	100
C_{33}	269.5	240	220	190	170
e_{31} (C/m^2)	0	-2	-3	-3.5	-4
e_{33}	0	4	7	11	14
q_{31} (N/Am)	580	410	300	200	100
q_{33}	700	550	380	260	120
k_{11} $(10^{-9}\ C/Vm)$	0.08	0.33	0.8	0.9	1
k_{33}	0.093	2.5	5	7.5	10
d_{11} $(10^{-12}\ Ns/VC)$	0	2.8	4.8	6	6.8
d_{33}	0	2000	2750	2500	1500
x_{11} $(10^{-4}\ Ns^2/C^2)$	-5.9	-3.9	-2.5	-1.5	-0.8
x_{33}	1.57	1.33	1	0.75	0.5
ρ (kg/m^3)	5300	5400	5500	5600	5700

magnetic permeability properties.

3. Shells made of multi-phase MEE material

In order to develop nonlinear formulation for nonlinear vibrations of the nanobeam, well-known classical beam theory has been used in the present paper. Thus, the displacements of nanobeam (u_1, $u_2 = 0$, u_3) may be written based on axial (u) and transverse (w) field variables as

$$u_1(x,y,z,t) = u(x,y,t) - z\frac{\partial w}{\partial x} \tag{1}$$

$$u_3(x,y,z,t) = w(x,y,t) \tag{2}$$

For the classic beam model, the strain field including geometric imperfection deflection (w^*) might be expressed by

$$\varepsilon_{xx} = \frac{\partial u_1}{\partial x} = \frac{\partial u}{\partial x} - z\frac{\partial^2 w}{\partial x^2} + \frac{1}{2}(\frac{\partial w}{\partial x})^2 + \frac{\partial w}{\partial x}\frac{\partial w^*}{\partial x} \tag{3}$$

Considering the fact that METE nanobeam is under electro-magnetic field with electrical potential (Φ) and magnetic potential (Υ), one can define the potentials in following forms as functions of electrical voltage (V_E) and magnetic potential intensity (Ω) (Ebrahimi and Barati 2016)

$$\Phi(x,y,z,t) = -cos(\beta z)\phi(x,y,t) + \frac{2z}{h}V \tag{4}$$

$$\Upsilon(x,y,z,t) = -\cos(\beta z)\gamma(x,y,t) + \frac{2z}{h}\Omega \tag{5}$$

with $\beta = \pi/h$. Calculating the two-dimensional gradient of electro-magnetic potentials gives the electrical field components (E_x, E_z) and magnet field components (H_x, H_z) as follows

$$E_x = -\Phi_{,x} = \cos(\beta z)\frac{\partial \phi}{\partial x}, \quad E_z = -\Phi_{,z} = -\beta \sin(\beta z)\phi - \frac{2V}{h} \tag{6}$$

$$H_x = -\Upsilon_{,x} = \cos(\beta z)\frac{\partial \gamma}{\partial x}, \quad H_z = -\Upsilon_{,z} = -\beta \sin(\beta z)\gamma - \frac{2\Omega}{h} \tag{7}$$

For a METE nano-size beam, the governing equations based on classic beam theory and nonlocal stress effects may be expressed by (Ke and Wang 2014)

$$\frac{\partial N_x}{\partial x} = I_0 \frac{\partial^2 u}{\partial t^2} - I_1 \frac{\partial^3 w}{\partial x \partial t^2} \tag{8}$$

$$\begin{aligned} &\frac{\partial^2 M_x}{\partial x^2} + \frac{\partial}{\partial x}\left(N_x\left[\frac{\partial w}{\partial x} + \frac{\partial w^*}{\partial x}\right]\right) - k_L w + k_P \frac{\partial^2 w}{\partial x^2} - k_{NL} w^3 \\ &= I_0 \frac{\partial^2 w}{\partial t^2} + I_1\left(\frac{\partial^3 u}{\partial x \partial t^2}\right) - I_2 \nabla^2\left(\frac{\partial^2 w}{\partial t^2}\right) \end{aligned} \tag{9}$$

$$\int_{-h/2}^{h/2}\left(\cos(\beta z)\frac{\partial D_x}{\partial x} + \beta \sin(\beta z) D_z\right) dz = 0 \tag{10}$$

$$\int_{-h/2}^{h/2}\left(\cos(\beta z)\frac{\partial B_x}{\partial x} + \beta \sin(\beta z) B_z\right) dz = 0 \tag{11}$$

in which D_i, B_i represent the components for electric and magnetic field displacements; k_L, k_P, K_{NL} are linear, shear and nonlinear layers of elastic substrate. Also, N_x and M_x are in-plane forces and bending moments defined by

$$(N_x, M_x) = \int_A (1, z, f)\sigma_x \, dA \tag{12}$$

so that

$$(I_0, I_1, I_2) = \int_{-h/2}^{h/2} (1, z \ \ , z^2)\rho \, dz \tag{13}$$

Note that the material is isotropic, then $I_1 = 0$. Next, the edge conditions would be

$$N_x = 0 \quad \text{or} \quad u = 0 \tag{14}$$

$$\frac{\partial M_x}{\partial x} + N_x\left[\frac{\partial w}{\partial x} + \frac{\partial w^*}{\partial x}\right] = 0 \qquad \text{or} \qquad w = 0 \tag{15}$$

$$\int_{-h/2}^{h/2} cos(\beta z) D_x dz = 0 \qquad \text{or} \qquad \phi = 0 \tag{16}$$

$$\int_{-h/2}^{h/2} cos(\beta z) B_x dz = 0 \qquad \text{or} \qquad \gamma = 0 \tag{17}$$

All ingredients of stress field, electrical field displacement (D_x, D_z) and magnetic induction (B_x, B_z) for a size-dependent beam relevant to nonlocal theory may be written as (Ebrahimi and Barati 2016)

$$(1-(ea)^2\nabla^2)\sigma_{xx} = \tilde{c}_{11}(\varepsilon_{xx} - \tilde{\alpha}\Delta T) - \tilde{e}_{31}E_z - \tilde{q}_{31}H_z \tag{18}$$

$$(1-(ea)^2\nabla^2)D_x = \tilde{e}_{15}\gamma_{xz} + \tilde{k}_{11}E_x + \tilde{d}_{11}H_x \tag{19}$$

$$(1-(ea)^2\nabla^2)D_z = \tilde{e}_{31}\varepsilon_{xx} + \tilde{k}_{33}E_z + \tilde{d}_{33}H_z \tag{20}$$

$$(1-(ea)^2\nabla^2)B_x = \tilde{q}_{15}\gamma_{xz} + \tilde{d}_{11}E_x + \tilde{\chi}_{11}H_x \tag{21}$$

$$(1-(ea)^2\nabla^2)B_z = \tilde{q}_{31}\varepsilon_{xx} + \tilde{d}_{33}E_z + \tilde{\chi}_{33}H_z \tag{22}$$

So that *ea* is nonlocal scale factor; ΔT is temperature rise. Elastic, piezoelectric and magnetic material characteristics have been respectively marked by C_{ij}, e_{ij} and q_{ij}. For considering plane stress conditions, all material properties are expressed in a new form a follows (Ke and Wang 2014)

$$\begin{aligned}
&\tilde{c}_{11} = c_{11} - \frac{c_{13}^2}{c_{33}}, \quad \tilde{c}_{12} = c_{12} - \frac{c_{13}^2}{c_{33}}, \quad \tilde{c}_{66} = c_{66}, \\
&\tilde{e}_{15} = e_{15}, \quad \tilde{e}_{31} = e_{31} - \frac{c_{13}e_{33}}{c_{33}}, \quad \tilde{q}_{15} = q_{15}, \quad \tilde{q}_{31} = q_{31} - \frac{c_{13}q_{33}}{c_{33}}, \\
&\tilde{d}_{11} = \tilde{d}_{11}, \quad \tilde{d}_{33} = \tilde{d}_{33} + \frac{q_{33}e_{33}}{c_{33}}, \quad \tilde{k}_{11} = k_{11}, \quad \tilde{k}_{33} = k_{33} + \frac{e_{33}^2}{c_{33}}, \\
&\tilde{\chi}_{11} = \chi_{11}, \quad \tilde{\chi}_{33} = \chi_{33} + \frac{q_{33}^2}{c_{33}}, \quad \tilde{\alpha} = \alpha_1 - \frac{c_{13}\alpha_3}{c_{33}}
\end{aligned} \tag{23}$$

By integration Eqs. (18)-(22) through the thickness direction, the below resultants for the nano-size beam would be derived

$$\begin{aligned}
(1-(ea)^2\nabla^2)N_x = A_{11}\left(\frac{\partial u}{\partial x} + \frac{1}{2}\left(\frac{\partial w}{\partial x}\right)^2 + \frac{\partial w}{\partial x}\frac{\partial w^*}{\partial x}\right) - B_{11}\frac{\partial^2 w}{\partial x^2} \\
+A_{31}^e\phi + A_{31}^m\gamma - N_x^E - N_x^H - N^T
\end{aligned} \tag{24}$$

$$(1-(ea)^2\nabla^2)M_x = B_{11}(\frac{\partial u}{\partial x}+\frac{1}{2}(\frac{\partial w}{\partial x})^2+\frac{\partial w}{\partial x}\frac{\partial w^*}{\partial x}) \\ -D_{11}\frac{\partial^2 w}{\partial x^2}+E_{31}^e\phi+E_{31}^m\gamma-M_x^E-M_x^H \tag{25}$$

$$\int_{-h/2}^{h/2}(1-(ea)^2\nabla^2)D_x\,cos(\beta z)dz = F_{11}^e\frac{\partial\phi}{\partial x}+F_{11}^m\frac{\partial\gamma}{\partial x} \tag{26}$$

$$(1-(ea)^2\nabla^2)\int_{-\frac{h}{2}}^{\frac{h}{2}}D_z\beta\,sin(\beta z)dz \\ =A_{31}^e\left(\left(\frac{\partial u}{\partial x}+\frac{1}{2}\frac{\partial w}{\partial x}\right)^2+\frac{\partial w}{\partial x}\frac{\partial w^*}{\partial x}\right)-E_{31}^e\frac{\partial^2 w}{\partial x^2}-F_{33}^e\phi-F_{33}^m\gamma \tag{27}$$

$$\int_{-h/2}^{h/2}(1-(ea)^2\nabla^2)B_x\,cos(\beta z)dz = +F_{11}^m\frac{\partial\phi}{\partial x}+X_{11}^m\frac{\partial\gamma}{\partial x} \tag{28}$$

$$\int_{-\frac{h}{2}}^{\frac{h}{2}}(1-(ea)^2\nabla^2)B_z\beta\,sin(\beta z)dz \\ =A_{31}^m\left(\frac{\partial u}{\partial x}+\frac{1}{2}\left(\frac{\partial w}{\partial x}\right)^2+\frac{\partial w}{\partial x}\frac{\partial w^*}{\partial x}\right)-E_{31}^m\nabla^2 w-F_{33}^m\phi-X_{33}^m\gamma \tag{29}$$

in which

$$\{A_{11},B_{11},D_{11}\}=\int_{-h/2}^{h/2}\tilde{c}_{11}(1,z,z^2)\,dz \tag{30}$$

$$\{A_{31}^e,E_{31}^e\}=\int_{-h/2}^{h/2}\tilde{e}_{31}\beta\,sin(\beta z)\{1,z\}\,dz \tag{31}$$

$$\{A_{31}^m,E_{31}^m\}=\int_{-h/2}^{h/2}\tilde{q}_{31}\beta\,sin(\beta z)\{1,z\}\,dz \tag{32}$$

$$\{F_{11}^e,F_{33}^e\}=\int_{-h/2}^{h/2}\left\{\tilde{k}_{11}\,cos^2(\beta z),\tilde{k}_{33}\beta^2\,sin^2(\beta z)\right\}dz \tag{33}$$

$$\{F_{11}^m,F_{33}^m\}=\int_{-h/2}^{h/2}\left\{\tilde{d}_{11}\,cos^2(\beta z),\tilde{d}_{33}\beta^2\,sin^2(\beta z)\right\}dz \tag{34}$$

$$\{X_{11}^m,X_{33}^m\}=\int_{-h/2}^{h/2}\{\tilde{\chi}_{11}\,cos^2(\beta z),\tilde{\chi}_{33}\beta^2\,sin^2(\beta z)\}\,dz \tag{35}$$

Moreover, electric, magnetic and thermal (N^T) fields exerts in-plane loads and moments which exist in Eqs. (24)-(25) as

$$N_x^E = -\int_{-\frac{h}{2}}^{\frac{h}{2}} \tilde{e}_{31}\frac{2V}{h}dz, \qquad N_x^H = -\int_{-\frac{h}{2}}^{\frac{h}{2}} \tilde{q}_{31}\frac{2\Omega}{h}dz, \qquad N^T = \int_{-h/2}^{h/2} \tilde{\alpha}\tilde{c}_{11}\Delta T dz \tag{36}$$

$$M_x^E = -\int_{-\frac{h}{2}}^{\frac{h}{2}} \tilde{e}_{31}\frac{2V}{h}zdz, \qquad M_x^H = -\int_{-h/2}^{h/2} \tilde{q}_{31}\frac{2\Omega}{h}zdz \tag{37}$$

The governing equations for a multi-phase nano-scale beam based upon displacement components would be obtained by inserting Eqs. (24)-(29), into Eqs. (8)-(11) as

$$A_{11}\left(\frac{\partial^2 u}{\partial x^2}+\frac{\partial w}{\partial x}\frac{\partial^2 w}{\partial x^2}+\frac{\partial^2 w}{\partial x^2}\frac{\partial w^*}{\partial x}+\frac{\partial w}{\partial x}\frac{\partial^2 w^*}{\partial x^2}\right)-B_{11}\frac{\partial^3 w}{\partial x^3}+A_{31}^e\frac{\partial \phi}{\partial x}+A_{31}^m\frac{\partial \gamma}{\partial x}=0 \tag{38}$$

$$\begin{aligned}&-D_{11}\frac{\partial^4 w}{\partial x^4}+E_{31}^e\left(\frac{\partial^2 \phi}{\partial x^2}\right)+E_{31}^m\left(\frac{\partial^2 \gamma}{\partial x^2}\right)+(1-(ea)^2\nabla^2)\left(-I_0\frac{\partial^2 w}{\partial t^2}-I_1\left(\frac{\partial^3 u}{\partial x \partial t^2}\right)+I_2\left(\frac{\partial^4 w}{\partial x^2 \partial t^2}\right)\right.\\&\left.+\left(A_{11}\left(\frac{\partial u}{\partial x}+\frac{1}{2}\left(\frac{\partial w}{\partial x}\right)^2+\frac{\partial w}{\partial x}\frac{\partial w^*}{\partial x}\right)-B_{11}\frac{\partial^2 w}{\partial x^2}+A_{31}^e\phi+A_{31}^m\gamma-N_x^E-N_x^H-N^T\right)\right.\\&\left.-k_L w+k_P\frac{\partial^2 w}{\partial x^2}-k_{NL}w^3\right)\left[\frac{\partial^2 w}{\partial x^2}+\frac{\partial^2 w^*}{\partial x^2}\right]=0\end{aligned} \tag{39}$$

$$A_{31}^e\left(\frac{\partial u}{\partial x}+\frac{1}{2}\left(\frac{\partial w}{\partial x}\right)^2+\frac{\partial w}{\partial x}\frac{\partial w^*}{\partial x}\right)-E_{31}^e\left(\frac{\partial^2 w}{\partial x^2}\right)+F_{11}^e\left(\frac{\partial^2 \phi}{\partial x^2}\right)+F_{11}^m\left(\frac{\partial^2 \gamma}{\partial x^2}\right)-F_{33}^e\phi-F_{33}^m\gamma=0 \tag{40}$$

$$A_{31}^m\left(\frac{\partial u}{\partial x}+\frac{1}{2}\left(\frac{\partial w}{\partial x}\right)^2+\frac{\partial w}{\partial x}\frac{\partial w^*}{\partial x}\right)-E_{31}^m\left(\frac{\partial^2 w}{\partial x^2}\right)+F_{11}^m\left(\frac{\partial^2 \phi}{\partial x^2}\right)+X_{11}^m\left(\frac{\partial^2 \gamma}{\partial x^2}\right)-F_{33}^m\phi-X_{33}^m\gamma=0 \tag{41}$$

An important conclusion from Eq. (38) is

$$A_{11}\left(\frac{\partial u}{\partial x}+\frac{1}{2}\left(\frac{\partial w}{\partial x}\right)^2+\frac{\partial w}{\partial x}\frac{\partial w^*}{\partial x}\right)+A_{31}^e\phi+A_{31}^m\gamma-N_x^E-N_x^H-N^T=C_1 \tag{42}$$

Then

$$\frac{\partial u}{\partial x}=-\frac{1}{2}\left(\frac{\partial w}{\partial x}\right)^2-\frac{\partial w}{\partial x}\frac{\partial w^*}{\partial x}-\frac{A_{31}^e}{A_{11}}\phi-\frac{A_{31}^m}{A_{11}}\gamma+\frac{N_x^E}{A_{11}}+\frac{N_x^H}{A_{11}}+\frac{N^T}{A_{11}}+\frac{C_1}{A_{11}} \tag{43}$$

Now, integrating Eq.(43) yields

$$\begin{aligned}u=&-\frac{1}{2}\int_0^x\left(\frac{\partial w}{\partial x}\right)^2dx-\int_0^x\frac{\partial w}{\partial x}\frac{\partial w^*}{\partial x}dx-\frac{A_{31}^e}{A_{11}}\int_0^x\phi\,dx-\frac{A_{31}^m}{A_{11}}\int_0^x\gamma\,dx+\frac{N_x^E}{A_{11}}\int_0^x dx\\&+\frac{N_x^H}{A_{11}}\int_0^x dx+\frac{N^T}{A_{11}}\int_0^x dx+\frac{C_1}{A_{11}}x+C_2\end{aligned} \tag{44}$$

Next, by considering boundary conditions $u(0) = 0$, $u(L) = 0$ the two constants would be obtained

$$\begin{aligned} C_2 &= 0 \\ C_1 &= \frac{A_{11}}{2L}\int_0^L (\frac{\partial w}{\partial x})^2\,dx + \frac{A_{11}}{L}\int_0^L \frac{\partial w}{\partial x}\frac{\partial w^*}{\partial x}dx + \frac{A_{31}^e}{L}\int_0^L \phi\,dx \\ &\quad + \frac{A_{31}^m}{L}\int_0^L \gamma\,dx - (N_x^E + N_x^H + N^T) \end{aligned} \tag{45}$$

The final governing equations for the METE nano-size beam will be derived after placing Eq. (43) in Eqs. (39)-(41) as

$$\begin{aligned} &-D_{11}\frac{\partial^4 w}{\partial x^4} + E_{31}^e(\frac{\partial^2 \phi}{\partial x^2}) + E_{31}^m(\frac{\partial^2 \gamma}{\partial x^2}) + (1-(ea)^2\nabla^2)(-I_0\frac{\partial^2 w}{\partial t^2} - I_1(\frac{\partial^3 u}{\partial x \partial t^2}) + I_2(\frac{\partial^4 w}{\partial x^2 \partial t^2}) \\ &+\left(A_{11}(+\frac{1}{2L}\int_0^L (\frac{\partial w}{\partial x})^2\,dx + \frac{1}{L}\int_0^L \frac{\partial w}{\partial x}\frac{\partial w^*}{\partial x}dx) - B_{11}\frac{\partial^2 w}{\partial x^2} - N_x^E - N_x^H - N^T\right) \\ &-k_L w + k_P\frac{\partial^2 w}{\partial x^2} - k_{NL}w^3)[\frac{\partial^2 w}{\partial x^2} + \frac{\partial^2 w^*}{\partial x^2}] = 0 \end{aligned} \tag{46}$$

$$\begin{aligned} &A_{31}^e(-\frac{A_{31}^e}{A_{11}}\phi - \frac{A_{31}^m}{A_{11}}\gamma + \frac{1}{2L}\int_0^L (\frac{\partial w}{\partial x})^2\,dx + \frac{1}{L}\int_0^L \frac{\partial w}{\partial x}\frac{\partial w^*}{\partial x}dx) - E_{31}^e(\frac{\partial^2 w}{\partial x^2}) + F_{11}^e(\frac{\partial^2 \phi}{\partial x^2}) \\ &+F_{11}^m(\frac{\partial^2 \gamma}{\partial x^2}) - F_{33}^e\phi - F_{33}^m\gamma = 0 \end{aligned} \tag{47}$$

$$\begin{aligned} &A_{31}^m(-\frac{A_{31}^e}{A_{11}}\phi - \frac{A_{31}^m}{A_{11}}\gamma + \frac{1}{2L}\int_0^L (\frac{\partial w}{\partial x})^2\,dx + \frac{1}{L}\int_0^L \frac{\partial w}{\partial x}\frac{\partial w^*}{\partial x}dx) - E_{31}^m(\frac{\partial^2 w}{\partial x^2}) + F_{11}^m(\frac{\partial^2 \phi}{\partial x^2}) \\ &+X_{11}^m(\frac{\partial^2 \gamma}{\partial x^2}) - F_{33}^m\phi - X_{33}^m\gamma = 0 \end{aligned} \tag{48}$$

4. Method of solution

The governing equation for METE nano-size beam only contains three displacements which need to be approximated based on following assumption (Ebrahimi and Barati 2016)

$$w = \sum_{i=1}^{\infty} W_m(t)X_i(x) \tag{49}$$

$$\phi = \sum_{i=1}^{\infty} \Phi_m(t)X_i(x) \tag{50}$$

$$\gamma = \sum_{i=1}^{\infty} \Upsilon_m(t)X_i(x) \tag{51}$$

where (W_{bmn} ,Φ_{mn},γ_{mn}) are the unknown coefficients and the function $X_m$defines a test function for considering edge conditions; $X_i = Sin(i\pi x/L)$ for simply supported conditions at both ends and $X_i = 0.5(1 - cos(2i\pi x/L))$ for clamped-clamped edges.

Then, the imperfection shape is considered as first buckling mode of the nano-size beam as

$$w^* = \sum_{i=1}^{\infty} W^*(t)F_i(x) \tag{52}$$

in which W^* defines the imperfections amplitude and F_i defines the shape functions for imperfections. Placing Eqs. (49)-(52) into Eqs. (46)-(48) gives three equations as

$$\begin{aligned} &K_1^S W_m + G_1 W_m^3 + Q_1 W_m^2 + M\ddot{W}_m + K_1^E \Phi_m + K_1^H \Upsilon_m + \Psi_1 W^* = 0 \\ &K_2^S W_m + G_2 W_m^2 + K_2^E \Phi_m + K_2^H \Upsilon_m = 0 \\ &K_3^S W_m + G_3 W_m^2 + K_3^E \Phi_m + K_3^H \Upsilon_m = 0 \end{aligned} \tag{53}$$

in which

$$\begin{aligned} K_1^S = &-D_{11}(\Lambda_{40}) - k_w \Lambda_{00} + k_p \Lambda_{20} - (N_x^E + N_x^H + N^T)\Lambda_{20} \\ &+(ea)^2(N_x^E + N_x^H + N^T)\Lambda_{40} + \frac{A_{11}}{L}\Xi_{11}\Gamma_{20}W^{*2} - (ea)^2\frac{A_{11}}{L}\Xi_{11}\Gamma_{40}W^{*2} \end{aligned} \tag{54}$$

$$\begin{aligned} G_1 &= \frac{A_{11}}{2L}\Lambda_{11}\Lambda_{20} - (ea)^2\frac{A_{11}}{2L}\Lambda_{11}\Lambda_{40} - k_{nl}(\Lambda_{0000} - (ea)^2(\Lambda_{1100} + \Lambda_{2000})) \\ Q_1 &= \frac{A_{11}}{2L}\Lambda_{11}\Gamma_{20}W^* - (ea)^2\frac{A_{11}}{2L}\Lambda_{11}\Gamma_{40}W^* + \frac{A_{11}}{L}\Xi_{11}\Lambda_{20}W^* - (ea)^2\frac{A_{11}}{L}\Xi_{11}\Lambda_{40}W^* \end{aligned} \tag{55}$$

$$K_1^E = E_{31}^e \Lambda_{20} \tag{56}$$

$$K_1^H = E_{31}^m \Lambda_{20} \tag{57}$$

$$K_2^S = -E_{31}^e \Lambda_{20} + \frac{A_{31}^e}{L}\Lambda_0 \Xi_{11} W^* \tag{58}$$

$$K_3^S = -E_{31}^m \Lambda_{20} + \frac{A_{31}^m}{L}\Lambda_0 \Xi_{11} W^* \tag{59}$$

$$G_2 = \frac{A_{31}^e}{2L}\Lambda_0 \Lambda_{11} \tag{60}$$

$$G_3 = \frac{A_{31}^m}{2L}\Lambda_0 \Lambda_{11} \tag{61}$$

$$K_2^E = -\frac{(A_{31}^e)^2}{A_{11}}\Lambda_{00} + F_{11}^e \Lambda_{20} - F_{33}^e \Lambda_{00} \tag{62}$$

$$K_2^H = -\frac{A_{31}^e A_{31}^m}{A_{11}}\Lambda_{00} + F_{11}^m \Lambda_{20} - F_{33}^m \Lambda_{00} \tag{63}$$

$$K_3^E = -\frac{A_{31}^e A_{31}^m}{A_{11}} \Lambda_{00} + F_{11}^m \Lambda_{20} - F_{33}^m \Lambda_{00} \tag{64}$$

$$K_3^H = -\frac{(A_{31}^m)^2}{A_{11}} \Lambda_{00} + X_{11}^m \Lambda_{20} - X_{33}^m \Lambda_{00} \tag{65}$$

$$\Psi_1 = -(N_x^E + N_x^H + N^T)\Gamma_{20} + (ea)^2 (N_x^E + N_x^H + N^T)\Gamma_{40} \tag{66}$$

$$M = -I_0 \Lambda_{00} + (ea)^2 I_0 \Lambda_{20} + I_2 \Lambda_{20} - (ea)^2 I_2 \Lambda_{40} \tag{67}$$

where

$$\begin{aligned} &\Lambda_{00} = \int_0^L X_i X_i dx, \quad \Lambda_{20} = \int_0^L X_i^{''} X_i dx, \quad \Lambda_{40} = \int_0^L X_i^{''''} X_i dx, \quad \Lambda_{11} = \int_0^L X_i^{'} X_i^{'} dx \\ &\tilde{\Lambda}_{00} = \int_0^L (X_i)^4 dx, \quad \Xi_{11} = \int_0^L F_i^{'} X_i^{'} dx, \quad \Gamma_{20} = \int_0^L F_i^{''} F_i dx, \quad \Gamma_{40} = \int_0^L F_i^{''''} F_i dx \end{aligned} \tag{68}$$

By using last two relations of Eq. (53), one can derive the variables Φ_m and Υ_m as follows

$$\begin{aligned} &\Phi_m = Z_1 W_m + Z_2 W_m^2, \qquad \Upsilon_m = Z_3 W_m + Z_4 W_m^2 \\ &Z_1 = -\frac{\left(K_2^H K_3^S - K_3^H K_2^S\right)}{K_3^E K_2^H - K_2^E K_3^H}, \qquad Z_2 = -\frac{(G_3 K_2^H - G_2 K_3^H)}{K_3^E K_2^H - K_2^E K_3^H} \\ &Z_3 = -\frac{\left(K_3^E K_2^S - K_2^E K_3^S\right)}{K_3^E K_2^H - K_2^E K_3^H}, \qquad Z_4 = -\frac{+(G_2 K_3^E - G_3 K_2^E)}{K_3^E K_2^H - K_2^E K_3^H} \end{aligned} \tag{69}$$

Placing Eq.(69) in the first relation of Eq.(53) results in

$$\frac{K^*}{M} W_m + \frac{G_1}{M} W_m^3 + \frac{Z^*}{M} W_m^2 + \ddot{W}_m + \frac{\Psi_1}{M} W^* = 0 \tag{70}$$

where

$$K^* = K_1^S + K_1^E Z_1 + K_1^H Z_3, \qquad Z^* = K_1^E Z_2 + K_1^H Z_4 + Q_1 \tag{71}$$

Next, via performing harmonic balance technique (Besseghier *et al*. 2015), one can solve Eq. (70). Assuming that vibrations of a nano-size beam take place in positive and negative directions of *z* axis, Eq. (70) must be rewritten as

$$\frac{K^*}{M} W_m + \frac{G_1}{M} W_m^3 + \frac{Z^*}{M} W_m |W_m| + \ddot{W}_m + \frac{\Psi_1}{M} W^* = 0 \tag{72}$$

It is supposed that an approximate solution may be defined by (Besseghier *et al*. 2015, Li and Hu 2016)

$$W(t) = \widetilde{W} \quad cos(\omega t) \tag{73}$$

in which is $\widetilde{W}$ the maximum vibration amplitude. Next, Eq. (73) is placed into Eq. (72) to obtain the below equation

$$\begin{aligned}&\frac{K^*}{M}\widetilde{W}\,cos(\,\omega t)+\frac{G_1}{M}\big(\widetilde{W}\,cos(\,\omega t)\big)^3+\frac{Z^*}{M}\big(\widetilde{W}\,cos(\,\omega t)\big)\big|\big(\widetilde{W}\,cos(\,\omega t)\big)\big|\\&-\widetilde{W}\omega^2\,cos(\,\omega t)+\frac{\Psi_1}{M}W^*=0\end{aligned}\tag{74}$$

Next, the below function definitions may be used for further calculations

$$\begin{aligned}&|cos(\,\omega t)|=\frac{4}{\pi}\left[\frac{1}{2}+\frac{1}{3}cos(\,2\omega t)-\frac{1}{15}cos(\,4\omega t)+\ldots.\right]cos(\,\omega t)|cos(\,\omega t)|\\&=\frac{4}{\pi}\left[\frac{1}{2}cos(\,\omega t)+\frac{1}{3}cos(\,2\omega t)\,cos(\,\omega t)-\frac{1}{15}cos(\,4\omega t)\,cos(\,\omega t)+\ldots.\right]=\frac{8}{3\pi}cos(\,\omega t)\end{aligned}\tag{75}$$

By performing some calculations using above relations, Eq. (74) may be expressed as follows

$$cos(\,\omega t)\left[\frac{K^*}{M}\widetilde{W}+\frac{3}{4}\frac{G_1}{M}\widetilde{W}^3+\frac{8\widetilde{W}^2}{3\pi}\frac{Z^*}{M}-\widetilde{W}\omega^2\,cos(\,\omega t)\right]=0\tag{76}$$

From above equation, it is easy to express the nonlinear vibration frequency as

$$\omega_{NL}=\sqrt{\frac{K^*}{M}+\frac{3}{4}\frac{G_1}{M}(\widetilde{W})^2+\frac{8\widetilde{W}}{3\pi}\frac{Z^*}{M}}\tag{77}$$

Also, dimensionless quantities are selected as

$$K_L=k_L\frac{L^4}{D_{11}},\qquad K_p=k_p\frac{L^2}{D_{11}},\qquad K_{NL}=k_{NL}\frac{L^4}{A_{11}},\qquad \widetilde{\omega}=\omega L^2\sqrt{\frac{\rho A}{\tilde{c}_{11}I}},\qquad \mu=\frac{ea}{L}\tag{78}$$

5. Discussion on results

Discussions on nonlinear vibration behavior of METE nanobeams having geometrical imperfection have been presented in this chapter. The nanobeam's length has been selected as L = 10 nm. Due to the reason that there is no published study about vibrations of geometrically imperfect METE nano-size beams, the vibration frequencies have been verified with those for imperfect elastic nano-size beams without piezo-electrical and magnetic field effects. Table 2 represents the non-linear vibrational frequencies of a nano-dimension beam based upon diverse values for maximum vibrational amplitude and also imperfection amplitude (W* = 0, 0.1, 0.2, 0.3) comparing to those achieved by Li *et al*. (2018). It is obvious that presented result is identically the same as that achieved by Li *et al*. (2018). Another investigation is provided in Table 3 to compare obtained vibrational frequencies of perfect piezo-magnetic nano-size beams with the findings presented by Ke and Wang (2014) based on differential quadrature method (DQM). In this table, the frequencies are presented for various values of nonlocal parameter and a good agreement with previously obtained results is observed.

Table 2 Verification of non-linear vibrational frequency for perfect/imperfect nano-size beams

		W* = 0	**W* = 0.1**	**W* = 0.2**	**W* = 0.3**
$\widetilde{W}$ **= 0.2**	**Li *et al.* (2018)**	9.9065	9.9933	10.1276	10.3075
	Present	9.9065	9.9933	10.1276	10.3075
$\widetilde{W}$ **= 0.4**	**Li *et al.* (2018)**	10.0166	10.1636	10.3557	10.5904
	Present	10.0166	10.1636	10.3557	10.5904

Table 3 Verification of vibrational frequency for piezo-magnetic nano-scale beams with different non-local factors (V_E = 0, Ω = 0)

	μ = 0	μ = 0.1	μ = 0.2	μ = 0.3	μ = 0.4
Ke and Wang (2014)	3.7388	3.5670	3.1658	2.7209	2.3281
Present	3.7392	3.5675	3.1662	2.7212	2.3283

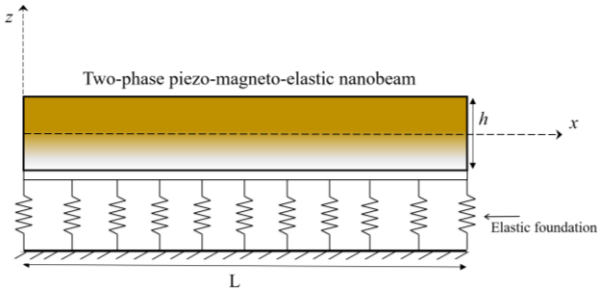

Fig. 1 Geometry of a piezoelectric-magnetic nano-scale beam

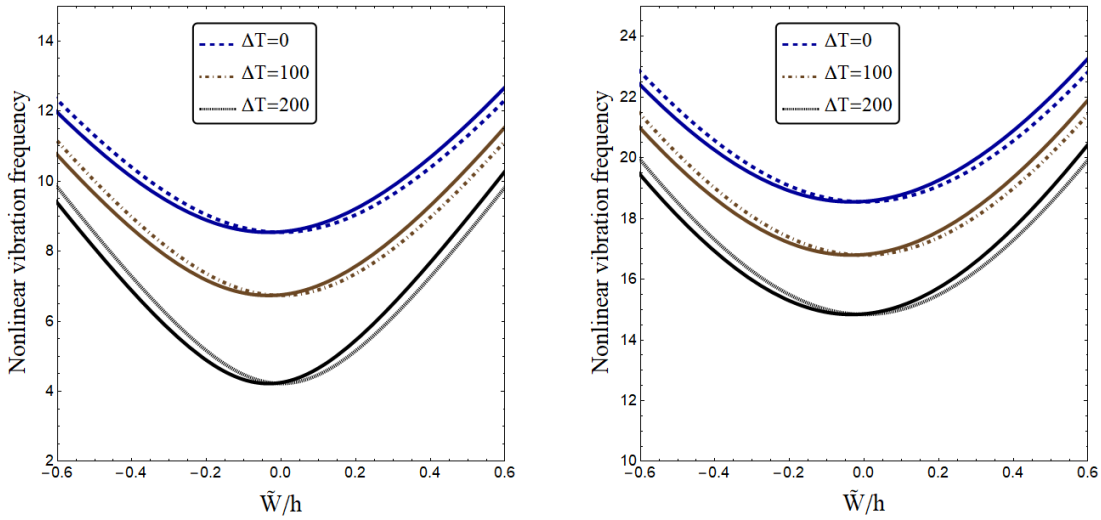

(a) S-S (b) C-C

Fig. 2 Non-linear frequency-amplitude curves of the nanobeam for various temperatures; dashed lines: perfect nanobeam, straight lines: imperfect nanobeam (L/h = 20, V_f = 20%, V_E = 0, Ω = 0, μ = 0.2, W*/h = 0.02)

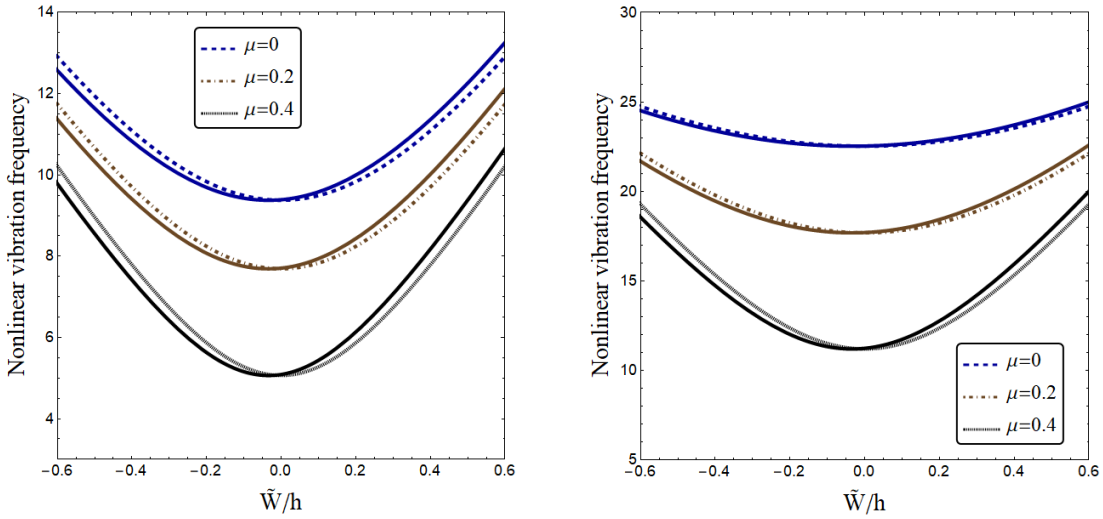

(a) S-S (b) C-C

Fig. 3 Non-linear frequency-amplitude curves of the nanobeam for various nonlocal parameters; dashed lines: perfect nanobeam, straight lines: imperfect nanobeam (ΔT = 50, V_f = 20%, V_E = 0, Ω = 0)

Temperature rise effects on nonlinear vibration curves of the nanobeam are shown in Fig. 2 when V_f = 20%. To this end, nonlinear vibration frequency is plotted versus normalized amplitude taking into account various value of temperature rise (ΔT). For oscillations in positive ($\widetilde{W}/h > 0$) and negative ($\widetilde{W}/h < 0$) directions, increasing in the value of normalized amplitude yields greater vibration frequencies for a perfect nanobeam owning to hardening impacts raised from geometric nonlinearities. In the case of a perfect nanobeam, the frequency-amplitude curves are symmetric with respect to $\widetilde{W}/h = 0$. However, the frequency-amplitude curves are not symmetric with respect to $\widetilde{W}/h = 0$ for an imperfect nanobeam. In fact, the nonlinear vibration frequency may decrease by increasing in the magnitude of dimensionless amplitude in the region of $\widetilde{W}/h < 0$. Also, temperature rise leads to lower nonlinear vibration frequency in both cases of ideal and non-ideal nano-scale beams.

Fig. 3 illustrates the nonlinear frequency-amplitude curves of the nanobeam for various nonlocal parameters with and without geometrical imperfections effects. For the figure, the piezoelectric constituent volume has been selected as V_f = 20%; exerted electrical voltage and magnetic potential have been assumed to be V_E = 0, Ω = 0. Simply supported-simply supported (S-S) and clamped-clamped (C-C) boundary conditions are considered for the nanobeam. For both perfect and imperfect nano-scale beams, the nonlinear frequency decreases as the nonlocality parameter increases, since the total stiffness of the nano-scale beam has been diminished. Thus, nonlocal stress field which captures wide range atomic interactions has a remarkable impact on vibration properties of geometrically imperfect piezoelectric-magnetic nano-scale beams.

Figs. 4 and 5 respectively show the influences of applied electrical voltages (V_E) and magnetic potential (Ω) on nonlinear vibration frequency of a smart nano-scale beam with/without geometric imperfections effects. The piezoelectric constituent volume has been considered as V_f = 20%. One can see that applying negative electrical voltages to a nano-scale beam causes greater nonlinear vibration frequencies than applying a positive electrical voltage. Such observation is because of

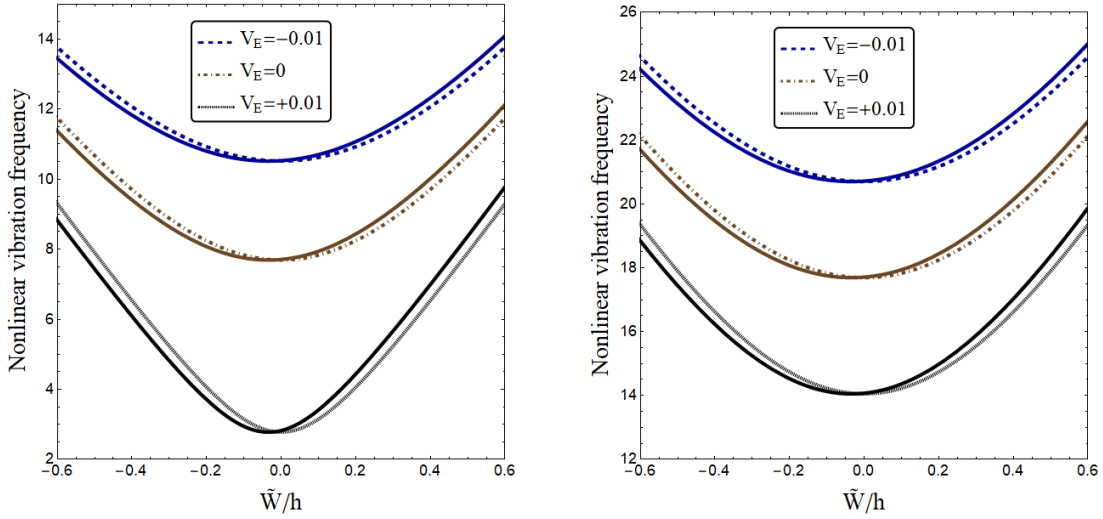

(a) S-S (b) C-C

Fig. 4 Non-linear frequency-amplitude curves of the nano-scale beam for different electrical voltages (V_f = 20%, μ = 0.2, Ω = 0, ΔT = 50)

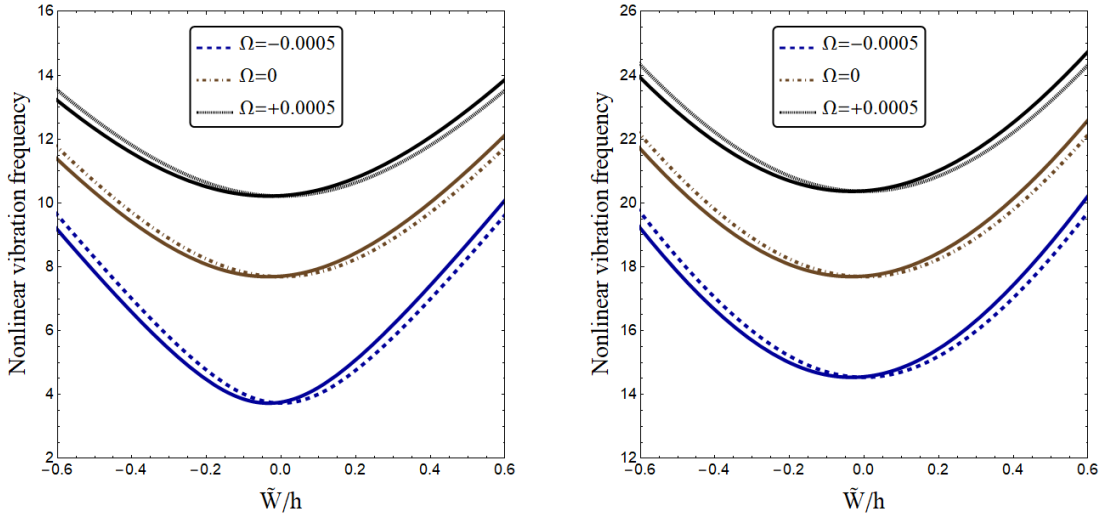

(a) S-S (b) C-C

Fig. 5 Non-linear frequency-amplitude curves of the nano-scale beam for different magnetic potentials (V_f = 20%, μ = 0.2, V_E = 0, ΔT = 50)

raised compressive loads by positive electrical voltages. Such compressive loadings might result in the decrement in structural stiffness of the nano-scale beam as well as vibration frequency. Another observation is that the effect of magnetic potentials on vibration frequency is in contrast to electrical voltages. Actually, negative magnetic potentials yield smaller nonlinear frequency than a positive one. Such observations are valid in both cases of ideal and non-ideal nano-scale

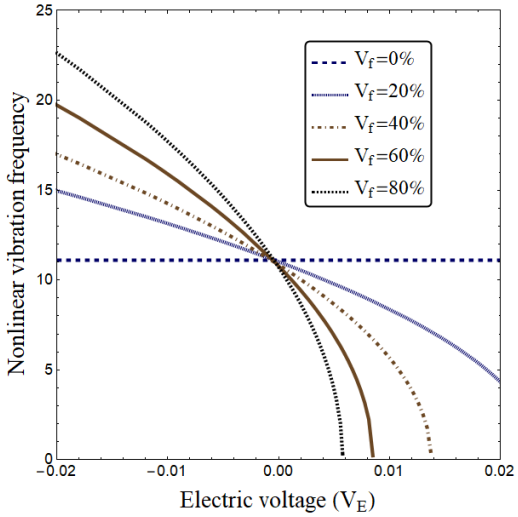

Fig. 6 Vibration frequency of imperfect nanobeam versus electrical voltage for different piezoelectric volume fractions (μ = 0.2, Ω = 0, $\widetilde{W}/h$ = 0.5, W*/h = 0.02, ΔT = 50)

beams. The new observation in this research is that when $\widetilde{W}/h < 0$, the nonlinear frequencies of an imperfect piezo-magnetic nano-scale beam diminishes at first and then increase with the rise of dimensionless amplitude, showing that there are both softening and hardening vibration behavior within a certain range of dimensionless amplitude.

Fig. 6 shows the variation of vibration frequency of a piezo-magnetic nano-scale beam versus exerted electrical voltages (V_E) according to diverse values for piezoelectric constituent volume(V_f). The geometrical imperfection magnitude and dimensionless vibration amplitude are

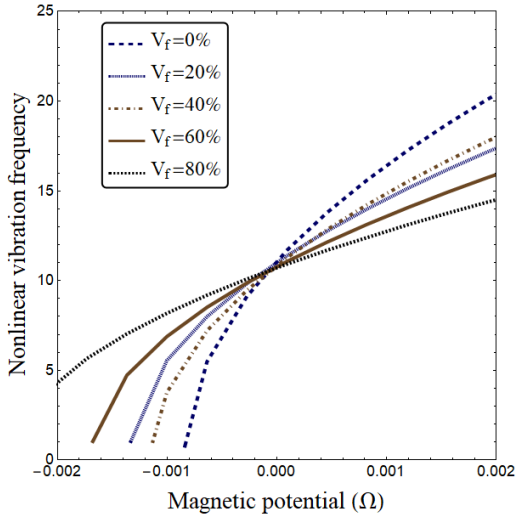

Fig. 7 Vibration frequency of imperfect nanobeam versus magnetic potentials for different piezoelectric volume fractions (μ = 0.2, V_E = 0, $\widetilde{W}/h$ = 0.5, W*/h = 0.02, ΔT = 50)

respectively considered as W*/h = 0.1 and $\widetilde{W}/h$ = 0.5. One may see that the vibration frequency stay constant by varying in electrical voltages at V_f = 0%. This is due to zero piezoelectric coefficient stated in Tale 1 when V_f = 0%. Thus, the nanobeam vibration is not dependent to electric voltages at zero volume of piezoelectric constituent. According to different values for V_f, varying the values of electrical voltages from negative to positive results in decrement in value of vibration frequency. The main conclusion from the figure is that the vibration frequency reduces via higher rates by increase of piezoelectric constituent volume. Thus, by increase of piezoelectric constituent volume the METE nanobeams become more susceptible to exerted electrical voltages.

Fig. 7 depicts the effects of piezo-electrical phase percentage (V_f) on the variation of vibrational frequency versus applied magnetic potential. One can see from the figure that for every value of piezoelectric phase percentage, the vibration frequency increases by changing the magnetic potential from negative to positive values. As can be seen, as the piezoelectric phase percentage increases, the sensibility of vibration frequency to magnetic field reduces. So, the rate of increment in vibration frequency with respect to magnetic potential reduces with the increase of piezoelectric constituent volume. As a conclusion, for a reliable design and analysis of two-phase smart nanobeams, it is necessary to select an appropriate amount of piezoelectric phase percentage to obtain their optimum vibration behavior in magneto-electric fields.

Fig. 8 shows the effect of geometric imperfection amplitude (W*/h) on non-linear vibration frequency of smart nanobeam having piezoelectric phase percentage of V_f = 20%. It is assumed that the nanobeam is exposed to an electric voltage of V_E = +0.01 and also a magnetic potential of Ω = 0.0005. It is seen from the figure that increasing geometric imperfection amplitude may increase the magnitude of vibration frequency. This is related to the energy stored in an imperfect nanobeam. Again, it can be observed that the nonlinear vibration characteristics of a smart nanobeam having geometrical imperfection largely depend on the vibration amplitude. In the case that $\widetilde{W}/h > 0$, increasing magnitudes of the dimensionless amplitude can increase the non-linear vibration frequency, highlighting the well-known “hard-spring” vibrational behavior. But in the

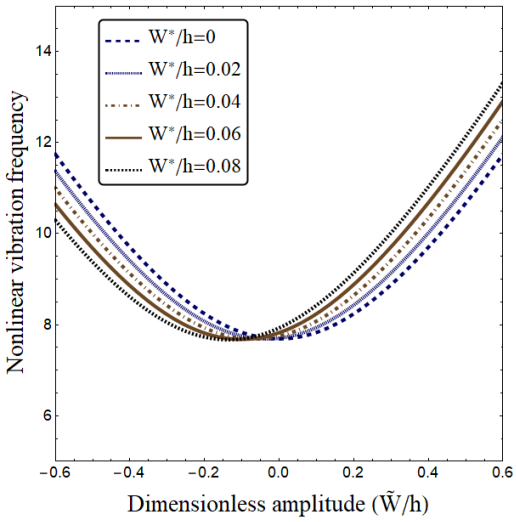

Fig. 8 Non-linear frequency-amplitude curves of the nano-scale beam for different geometric imperfections (V_f = 20%, μ = 0.2, V_E = 0, ΔT = 50)

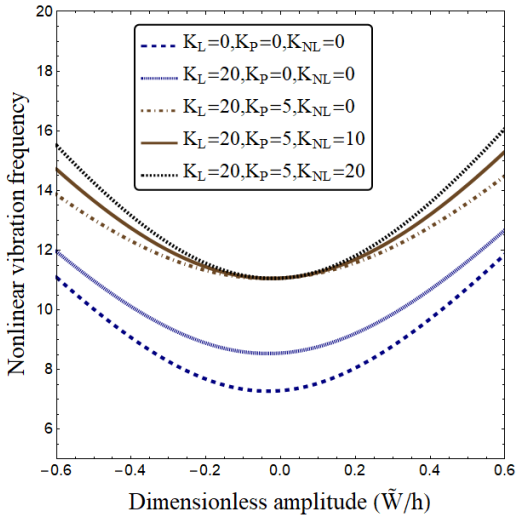

Fig. 9 Non-linear frequency-amplitude curves of imperfect nano-scale beam for different foundation parameters (V_f = 20%, μ = 0.2, V_E = 0.01, Ω = +0.0005, W*/h = 0.02, ΔT = 50)

range of negative vibration amplitudes, the non-linear vibrational frequency experiences both reduction and increment.

Fig. 9 indicates the effects of linear (K_L), shear (K_P) and nonlinear (K_{NL}) springs of elastic substrate on vibration characteristics of an imperfect smart nanobeam when the amplitude of imperfection is set to W*/h = 0.1. It is seen that increasing the magnitude of substrate coefficients makes the smart nanobeam stiffer leading to greater vibration frequencies. Also, hardening effect of the nonlinear substrate springs becomes more prominent as the magnitude of dimensionless amplitude ($\widetilde{W}/h$) increases in both positive and negative directions. But, it has no impact on vibration frequency at zero vibration amplitude. However, the influence of two other coefficients (K_L and K_P) on vibration frequency is not dependent on the magnitudes of vibration amplitudes.

6. Conclusions

An analysis of nonlinear free vibration behavior of smart two-phase magneto-electro-elastic nanoebeams having initial geometric imperfection was performed in this research. An analytical trend was proposed to obtain nonlinear vibration frequencies of such nanobeams for the first time. In the cases of ideal and imperfect smart nanobeams, growth of nonlocal factor led to smaller nonlinear frequencies. It was also seen that the nonlinear frequency of an imperfect piezo-magnetic nanobeam reduced at first and then increased with the rise of vibration amplitude, showing that there are both softening and hardening vibration behavior within a certain range of vibration amplitude. Also, by increase of piezoelectric constituent volume the METE nanobeams become more susceptible to exerted electrical voltages. However, the sensitivity of vibration frequency to magnetic potentials diminished by the increase of piezo-electrical constituent volume.

Acknowledgments

The authors would like to thank Mustansiriyah university (www.uomustansiriyah.edu.iq) Baghdad-Iraq for its support in the present work.

References

Aboudi, J. (2001), "Micromechanical analysis of fully coupled electro-magneto-thermo-elastic multiphase composites", *Smart Mater. Struct.*, **10**(5), 867. https://doi.org/10.1088/0964-1726/10/5/303

Ahmed, R.A., Fenjan, R.M. and Faleh, N.M. (2019), "Analyzing post-buckling behavior of continuously graded FG nanobeams with geometrical imperfections", *Geomech. Eng., Int. J.*, **17**(2), 175-180. https://doi.org/10.12989/gae.2019.17.2.175

Alzahrani, E.O., Zenkour, A.M. and Sobhy, M. (2013), "Small scale effect on hygro-thermo-mechanical bending of nanoplates embedded in an elastic medium", *Compos. Struct.*, **105**, 163-172. https://doi.org/10.1016/j.compstruct.2013.04.045

Annigeri, A.R., Ganesan, N. and Swarnamani, S. (2007), "Free vibration behaviour of multiphase and layered magneto-electro-elastic beam", *J. Sound Vib.*, **299**(1-2), 44-63. https://doi.org/10.1016/j.jsv.2006.06.044

Ansari, R., Ramezannezhad, H. and Gholami, R. (2012), "Nonlocal beam theory for nonlinear vibrations of embedded multiwalled carbon nanotubes in thermal environment", *Nonlinear Dyn.*, **67**(3), 2241-2254. https://doi.org/10.1007/s11071-011-0142-z

Ansari, R., Gholami, R and Rouhi, H. (2015), "Size-dependent nonlinear forced vibration analysis of magneto-electro-thermo-elastic Timoshenko nanobeams based upon the nonlocal elasticity theory", *Compos. Struct.*, **126**, 216-226. https://doi.org/10.1016/j.compstruct.2015.02.068

Arefi, M and Zenkour, A.M. (2016), "Employing sinusoidal shear deformation plate theory for transient analysis of three layers sandwich nanoplate integrated with piezo-magnetic face-sheets", *Smart Mater. Struct.*, **25**(11), 115040. https://doi.org/10.1088/0964-1726/25/11/115040

Azimi, M., Mirjavadi, S.S., Shafiei, N. and Hamouda, A.M.S. (2017), "Thermo-mechanical vibration of rotating axially functionally graded nonlocal Timoshenko beam", *Appl. Phys. A*, **123**(1), 104.

Azimi, M., Mirjavadi, S.S., Shafiei, N., Hamouda, A.M.S. and Davari, E. (2018), "Vibration of rotating functionally graded Timoshenko nano-beams with nonlinear thermal distribution", *Mech. Adv. Mater. Struct.*, **25**(6), 467-480. https://doi.org/10.1080/15376494.2017.1285455

Barati, M. R and Zenkour, A. (2017), "A general bi-Helmholtz nonlocal strain-gradient elasticity for wave propagation in nanoporous graded double-nanobeam systems on elastic substrate", *Compos. Struct.*, **168**, 885-892. https://doi.org/10.1016/j.compstruct.2017.02.090

Berrabah, H.M., Tounsi, A., Semmah, A. and Adda, B. (2013), "Comparison of various refined nonlocal beam theories for bending, vibration and buckling analysis of nanobeams", *Struct. Eng. Mech., Int. J.*, **48**(3), 351-365. https://doi.org/10.12989/sem.2013.48.3.351

Besseghier, A., Heireche, H., Bousahla, A.A., Tounsi, A. and Benzair, A. (2015), "Nonlinear vibration properties of a zigzag single-walled carbon nanotube embedded in a polymer matrix", *Adv. Nano Res., Int. J.*, **3**(1), 29-37. https://doi.org/10.12989/anr.2015.3.1.029

Besseghier, A., Houari, M.S.A., Tounsi, A and Mahmoud, S.R. (2017), "Free vibration analysis of mbedded nanosize FG plates using a new nonlocal trigonometric shear deformation theory", *Smart Struct. Syst., Int. J.*, **19**(6), 601-614. https://doi.org/10.12989/sss.2017.19.6.601

Bouafia, K., Kaci, A., Houari, M.S.A., Benzair, A. and Tounsi, A. (2017), "A nonlocal quasi-3D theory for bending and free flexural vibration behaviors of functionally graded nanobeams", *Smart Struct. Syst., Int. J.*, **19**(2), 115-126. https://doi.org/10.12989/sss.2017.19.2.115

Bounouara, F., Benrahou, K.H., Belkorissat, I. and Tounsi, A. (2016), "A nonlocal zeroth-order shear deformation theory for free vibration of functionally graded nanoscale plates resting on elastic foundation",

Steel Compos. Struct., Int. J., **20**(2), 227-249. https://doi.org/10.12989/scs.2016.20.2.227
Chen, C., Li, S., Dai, L. and Qian, C. (2014), "Buckling and stability analysis of a piezoelectric viscoelastic nanobeam subjected to van der Waals forces", *Commun. Nonlinear Sci. Numer. Simul.*, **19**(5), 1626-1637. https://doi.org/10.1016/j.cnsns.2013.09.017
Ebrahimi, F. and Barati, M.R. (2016), "A nonlocal higher-order refined magneto-electro-viscoelastic beam model for dynamic analysis of smart nanostructures", *Int. J. Eng. Sci.*, **107**, 183-196. https://doi.org/10.1016/j.ijengsci.2016.08.001
Ebrahimi, F. and Barati, M.R. (2017), "Magnetic field effects on dynamic behavior of inhomogeneous thermo-piezo-electrically actuated nanoplates", *J. Brazil. Soc. Mech. Sci. Eng.*, **39**(6), 2203-2223. https://doi.org/10.1007/s40430-016-0646-z
Ebrahimi, F., Mahmoodi, F. and Barati, M.R. (2017), "Thermo-mechanical vibration analysis of functionally graded micro/nanoscale beams with porosities based on modified couple stress theory", *Adv. Mater. Res., Int. J.*, **6**(3), 279-301. https://doi.org/10.12989/amr.2017.6.3.279
Eltaher, M.A., Emam, S.A. and Mahmoud, F.F. (2012), "Free vibration analysis of functionally graded size-dependent nanobeams", *Appl. Math. Computat.*, **218**(14), 7406-7420. https://doi.org/10.1016/j.amc.2011.12.090
Eltaher, M.A., Khater, M.E., Park, S., Abdel-Rahman, E. and Yavuz, M. (2016), "On the static stability of nonlocal nanobeams using higher-order beam theories", *Adv. Nano. Res., Int. J.*, **4**(1), 51-64. https://doi.org/10.12989/anr.2016.4.1.051
Eringen, A.C. (1972), "Linear theory of nonlocal elasticity and dispersion of plane waves", *Int. J. Eng. Sci.*, **10**(5), 425-435. https://doi.org/10.1016/0020-7225(72)90050-X
Fang, B., Zhen, Y.X., Zhang, C.P. and Tang, Y. (2013), "Nonlinear vibration analysis of double-walled carbon nanotubes based on nonlocal elasticity theory", *Appl. Math. Model.*, **37**(3), 1096-1107. https://doi.org/10.1016/j.apm.2012.03.032
Guo, J., Chen, J. and Pan, E. (2016), "Static deformation of anisotropic layered magnetoelectroelastic plates based on modified couple-stress theory", *Compos. Part B: Eng.*, **107**, 84-96. https://doi.org/10.1016/j.compositesb.2016.09.044
Jandaghian, A.A. and Rahmani, O. (2016), "Free vibration analysis of magneto-electro-thermo-elastic nanobeams resting on a Pasternak foundation", *Smart Mater. Struct.*, **25**(3), 035023. https://doi.org/10.1088/0964-1726/25/3/035023
Karličić, D., Kozić, P., Pavlović, R. and Nešić, N. (2017), "Dynamic stability of single-walled carbon nanotube embedded in a viscoelastic medium under the influence of the axially harmonic load", *Compos. Struct.*, **162**, 227-243. https:r//doi.org/10.1016/j.compstruct.2016.12.003
Karličić, D., Cajić, M. and Adhikari, S. (2018), "Dynamic stability of a nonlinear multiple-nanobeam system. *Nonlinear Dynamics*, **93**(3), 1495-1517. https://doi.org/10.1007/s11071-018-4273-3
Ke, L.L. and Wang, Y.S. (2014), "Free vibration of size-dependent magneto-electro-elastic nanobeams based on the nonlocal theory", *Physica E: Low-Dimens. Syst. Nanostruct.*, **63**, 52-61. https://doi.org/10.1016/j.physe.2014.05.002
Kumaravel, A., Ganesan, N. and Sethuraman, R. (2007), "Buckling and vibration analysis of layered and multiphase magneto-electro-elastic beam under thermal environment", *Multidiscipl. Model. Mater. Struct.*, **3**(4), 461-476. https://doi.org/10.1163/157361107782106401
Li, L. and Hu, Y. (2016), "Nonlinear bending and free vibration analyses of nonlocal strain gradient beams made of functionally graded material", *Int. J. Eng. Sci.*, **107**, 77-97. https://doi.org/10.1016/j.ijengsci.2016.07.011
Li, Y. and Shi, Z. (2009), "Free vibration of a functionally graded piezoelectric beam via state-space based differential quadrature", *Compos. Struct.*, **87**(3), 257-264. https://doi.org/10.1016/j.compstruct.2008.01.012
Li, L., Tang, H. and Hu, Y. (2018), "Size-dependent nonlinear vibration of beam-type porous materials with an initial geometrical curvature", *Compos. Struct.*, **184**, 1177-1188. https://doi.org/10.1016/j.compstruct.2017.10.052
Mashat, D.S., Zenkour, A.M. and Sobhy, M. (2016), "Investigation of vibration and thermal buckling of

nanobeams embedded in an elastic medium under various boundary conditions", *J. Mech.*, **32**(3), 277-287. https://doi.org/10.1017/jmech.2015.83

Mirjavadi, S.S., Afshari, B.M., Shafiei, N., Hamouda, A.M.S. and Kazemi, M. (2017), "Thermal vibration of two-dimensional functionally graded (2D-FG) porous Timoshenko nanobeams", *Steel Compos. Struct., Int. J.*, **25**(4), 415-426. https://doi.org/10.12989/scs.2017.25.4.415

Mirjavadi, S.S., Afshari, B.M., Barati, M.R. and Hamouda, A.M.S. (2018a), "Strain gradient based dynamic response analysis of heterogeneous cylindrical microshells with porosities under a moving load", *Mater. Res. Express*, **6**(3), 035029. https://doi.org/10.1088/2053-1591/aaf5a2

Mirjavadi, S.S., Afshari, B.M., Khezel, M., Shafiei, N., Rabby, S. and Kordnejad, M. (2018b), "Nonlinear vibration and buckling of functionally graded porous nanoscaled beams", *J. Brazil. Soc. Mech. Sci. Eng.*, **40**(7), 352. https://doi.org/10.1007/s40430-018-1272-8

Mirjavadi, S.S., Forsat, M., Hamouda, A.M.S. and Barati, M.R. (2019a), "Dynamic response of functionally graded graphene nanoplatelet reinforced shells with porosity distributions under transverse dynamic loads", *Mater. Res. Express*, **6**(7), 075045. https://doi.org/10.1088/2053-1591/ab1552

Mirjavadi, S.S., Forsat, M., Nikookar, M., Barati, M.R. and Hamouda, A.M.S. (2019b), "Nonlinear forced vibrations of sandwich smart nanobeams with two-phase piezo-magnetic face sheets", *Eur. Phys. J. Plus*, **134**(10), 508. https://doi.org/10.1140/epjp/i2019-12806-8

Mirjavadi, S.S., Afshari, B.M., Barati, M.R. and Hamouda, A.M.S. (2019c), "Transient response of porous FG nanoplates subjected to various pulse loads based on nonlocal stress-strain gradient theory", *Eur. J. Mech.-A/Solids*, **74**, 210-220. https://doi.org/10.1016/j.euromechsol.2018.11.004

Mirjavadi, S.S., Afshari, B.M., Barati, M.R. and Hamouda, A.M.S. (2019d), "Nonlinear free and forced vibrations of graphene nanoplatelet reinforced microbeams with geometrical imperfection", *Microsyst. Technol.*, **25**, 3137-3150. https://doi.org/10.1007/s00542-018-4277-4

Mirjavadi, S.S., Forsat, M., Barati, M.R., Abdella, G.M., Hamouda, A.M.S., Afshari, B.M. and Rabby, S. (2019e), "Post-buckling analysis of piezo-magnetic nanobeams with geometrical imperfection and different piezoelectric contents", *Microsyst. Technol.*, **25**(9), 3477-3488. https://doi.org/10.1007/s00542-018-4241-3

Mirjavadi, S.S., Forsat, M., Barati, M.R., Abdella, G.M., Afshari, B.M., Hamouda, A.M.S. and Rabby, S. (2019f), "Dynamic response of metal foam FG porous cylindrical micro-shells due to moving loads with strain gradient size-dependency", *Eur. Phys. J. Plus*, **134**(5), 214. https://doi.org/10.1140/epjp/i2019-12540-3

Nan, C.W. (1994), "Magnetoelectric effect in composites of piezoelectric and piezomagnetic phases", *Physical Review B*, **50**(9), 6082.

Pan, E and Han, F. (2005), "Exact solution for functionally graded and layered magneto-electro-elastic plates", *Int. J. Eng. Sci.*, **43**(3-4), 321-339. https://doi.org/10.1016/j.ijengsci.2004.09.006

Semmah, A., Beg, O.A., Mahmoud, S.R., Heireche, H. and Tounsi, A. (2014), "Thermal buckling properties of zigzag single-walled carbon nanotubes using a refined nonlocal model", *Adv. Mater. Res., Int. J.*, **3**(2), 77-89. https://doi.org/10.12989/amr.2014.3.2.077

Sobhy, M. (2014a), "Generalized two-variable plate theory for multi-layered graphene sheets with arbitrary boundary conditions", *Acta Mechanica*, **225**(9), 2521-2538. https://doi.org/10.1007/s00707-014-1093-5

Sobhy, M. (2014b), "Natural frequency and buckling of orthotropic nanoplates resting on two-parameter elastic foundations with various boundary conditions", *J. Mech.*, **30**(5), 443-453. https://doi.org/10.1017/jmech.2014.46

Sobhy, M. (2015), "Levy-type solution for bending of single-layered graphene sheets in thermal environment using the two-variable plate theory", *Int. J. Mech. Sci.*, **90**, 171-178. https://doi.org/10.1016/j.ijmecsci.2014.11.014

Sobhy, M. (2019), "Levy solution for bending response of FG carbon nanotube reinforced plates under uniform, linear, sinusoidal and exponential distributed loadings", *Eng. Struct.*, **182**, 198-212. https://doi.org/10.1016/j.engstruct.2018.12.071

Sobhy, M. and Abazid, M.A. (2019), "Dynamic and instability analyses of FG graphene-reinforced sandwich deep curved nanobeams with viscoelastic core under magnetic field effect", *Compos. Part B:*

Eng., 106966. https://doi.org/10.1016/j.compositesb.2019.106966
Sobhy, M. and Radwan, A.F. (2017), "A new quasi 3D nonlocal plate theory for vibration and buckling of FGM nanoplates", *Int. J. Appl. Mech*., **9**(1), 1750008. https://doi.org/10.1142/S1758825117500089
Sobhy, M. and Zenkour, A.M. (2018a), "Magnetic field effect on thermomechanical buckling and vibration of viscoelastic sandwich nanobeams with CNT reinforced face sheets on a viscoelastic substrate", *Compos. Part B*: *Eng*., **154**, 492-506. https://doi.org/10.1016/j.compositesb.2018.09.011
Sobhy, M. and Zenkour, A.M. (2018b), "The modified couple stress model for bending of normal deformable viscoelastic nanobeams resting on visco-Pasternak foundations", *Mech. Adv. Mater. Struct*., 1-14. https://doi.org/10.1080/15376494.2018.1482579
Sobhy, M. and Zenkour, A.M. (2018c), "Nonlocal thermal and mechanical buckling of nonlinear orthotropic viscoelastic nanoplates embedded in a visco-pasternak medium", *Int. J. Appl. Mech*., **10**(8), 1850086. https://doi.org/10.1142/S1758825118500862
Thai, H.T. and Vo, T.P. (2012), "A nonlocal sinusoidal shear deformation beam theory with application to bending, buckling, and vibration of nanobeams", *Int. J. Eng. Sci*., **54**, 58-66. https://doi.org/10.1016/j.ijengsci.2012.01.009
Zemri, A., Houari, M.S.A., Bousahla, A.A. and Tounsi, A. (2015), "A mechanical response of functionally graded nanoscale beam: an assessment of a refined nonlocal shear deformation theory beam theory", *Struct. Eng. Mech., Int. J*., **54**(4), 693-710.
Zenkour, A.M. and Sobhy, M. (2013), "Nonlocal elasticity theory for thermal buckling of nanoplates lying on Winkler–Pasternak elastic substrate medium", *Physica E*: *Low-dimens. Syst. Nanostruct*., **53**, 251-259. https://doi.org/10.1016/j.physe.2013.04.022
Zenkour, A.M. and Sobhy, M. (2015), "A simplified shear and normal deformations nonlocal theory for bending of nanobeams in thermal environment", *Phys. E*: *Low-Dimens. Syst. Nanostruct*., **70**, 121-128. https://doi.org/10.1016/j.physe.2015.02.022

CC